

## Apatite precipitation on a novel fast-setting calcium silicate cement containing fluoride

Bahram Ranjkesh<sup>a</sup>, Jacques Chevallier<sup>b</sup>, Hamideh Salehi<sup>c</sup>, Frédéric Cuisinier<sup>c</sup>, Flemming Isidor<sup>a</sup> and Henrik Løvschall<sup>a</sup>

<sup>a</sup>Department of Dentistry Health, Aarhus University, Aarhus C, Denmark; <sup>b</sup>Department of Physics and Astronomy, Aarhus University, Aarhus C, Denmark; <sup>c</sup>Bioengineering and Nanoscience Laboratory, UFR d'Odontologie, Université Montpellier 1, Montpellier, France

### ABSTRACT

**Aim:** Calcium silicate cements are widely used in endodontics. Novel fast-setting calcium silicate cement with fluoride (Protooth) has been developed for potential applications in teeth crowns including cavity lining and cementation.

**Objective:** To evaluate the surface apatite-forming ability of Protooth compositions as a function of fluoride content and immersion time in phosphate-buffered saline (PBS).

**Material and methods:** Three cement compositions were tested: Protooth (3.5% fluoride and 10% radiocontrast), ultrafast Protooth (3.5% fluoride and 20% radiocontrast), and high fluoride Protooth (15% fluoride and 25% radiocontrast). Powders were cap-mixed with liquid, filled to the molds and immersed in PBS. Scanning electron microscopy, energy dispersive X-ray analysis, and Raman spectroscopy were used to characterize the precipitations morphology and composition after 1, 7, 28, and 56 days. Apatite/belite Raman peak height indicated the apatite thickness.

**Results:** Spherical calcium phosphate precipitations with acicular crystallites were formed after 1-day immersion in PBS and Raman spectra disclosed the phosphate band at  $965\text{ cm}^{-1}$ , supporting the apatite formation over Protooth compositions. The apatite deposition continued and more voluminous precipitations were observed after 56 days over the surface of all cements. Raman bands suggested the formation of  $\beta$ -type carbonated apatite over Protooth compositions. High fluoride Protooth showed the most compact deposition with significantly higher apatite/belite ratio compared to Protooth and ultrafast Protooth after 28 and 56 days.

**Conclusions:** Calcium phosphate precipitations (apatite) were formed over Protooth compositions after immersion in PBS with increasing apatite formation as a function of time. High fluoride Protooth exhibited thicker apatite deposition.

### ARTICLE HISTORY

Received 13 February 2016  
Accepted 11 April 2016

### KEYWORDS

Apatite; calcium silicate cement; fluoride; mineral trioxide aggregate



## Introduction

Calcium silicate cements including mineral trioxide aggregates (MTA) are widely used in endodontic treatments. Calcium silicate cements have demonstrated apatite formation in physiological-like liquid,[1,2] superior sealing [3] and favorable bacteriostatic effect.[4] However, long setting time of MTA,[5] poor handling characteristics,[6] and the wash-out risk upon contact with liquid limit the practical usage in tooth crown.[7] Efforts have been made to shorten the setting time by adding different setting accelerators such as  $\text{Na}_2\text{HPO}_4$ ,[8] calcium lactate gluconate,[6] and calcium chloride [5,9] even in expense of mechanical properties.[5,10]

Calcium silicate cements are hydrophilic powders, which mix with water and set superiorly in humid condition in contrast to glass ionomers, which requires

protection against excessive humidity during setting.[11] The hydration products of calcium silicate cements are mainly calcium hydroxide (CH) and calcium silicate hydrate.[12] The high CH release reacts with available phosphate ions in physiological and biological environment, which forms calcium phosphate precipitations including apatite.[2] Long-term apatite formation on a material surface in simulated body fluid has been suggested to have favorable clinical effects.[13]

A novel fast-setting hydrophilic calcium silicate cement with fluoride called 'Protooth' has been developed to support mineralization. The novel cement is a candidate material for potential application similar to Dycal, IRM, glass ionomers, and zinc phosphate cement. Protooth consistency for usages can be changed according to the potential applications. The setting time

**CONTACT** Bahram Ranjkesh  [b.ranjkes@gmail.com](mailto:b.ranjkes@gmail.com)  Department of Dentistry, Health, Aarhus University, Vennelyst Boulevard 9, 8000 Aarhus C, Denmark

© 2016 The Author(s). Published by Informa UK Limited, trading as Taylor & Francis Group. This is an Open Access article distributed under the terms of the Creative Commons Attribution-NonCommercial License (<http://creativecommons.org/licenses/by-nc/4.0/>), which permits unrestricted non-commercial use, distribution, and reproduction in any medium, provided the original work is properly cited.)

of Protooth according to consistency is in the range of 4–10 minutes. Taken together, Protooth is a candidate dental material with potential preventive applications including cementation, cavity lining, traumatic tooth treatment, and endodontic complication. The aim of this study was to evaluate the surface apatite-forming ability of Protooth as a function of fluoride content and immersion time in phosphate-buffered saline (PBS).

## Material and methods

### Sample preparation

A novel calcium silicate cement (Protooth™, Dentosolve, Aarhus, Denmark) is comprised of tricalcium silicate, dicalcium silicate, tricalcium aluminate, calcium sulfate, fluoride, nanosilica, and radiopaque additive. The mixing liquid is water with 2% polycarboxylic acid as superplasticizer in order to enhance particle hydration and improve the mechanical properties.

Three cement compositions were tested in this study (Table 1): Protooth comprising 3.5% and 10% zirconium oxide as radiocontrast additive at creamy consistency (8–10 min setting time), (ii) ultrafast Protooth with marginal calcium sulfate/aluminate ratio adjustment providing ultrafast setting time (1½ to 2 min) at flowable consistency with 3.5% fluoride, 20% zirconium oxide, and (iii) high fluoride Protooth at clay condensable consistency (8–10 min setting time) with 15% fluoride (9% strontium fluoride) and 16% bismuth oxide.

One gram of each powder in different powder-to-liquid ratio was cap-mixed (CapMix™, 3M, ESPE, Seefeld, Germany) with hydration liquid for 20 seconds. After mixing, the paste was dispensed onto a plate and manually mixed briefly on glass slab to homogenize the slurry. Pastes were filled into molds with 6 mm diameter and 2 mm height with the exposed area of 28.26 mm<sup>2</sup>. A total of 12 samples for each group were prepared ( $n = 3$  per each time point). Each sample was immersed individually in a closed container with 10 ml PBS (PBS; 136.4 mmol/L NaCl, 2.7 mmol/L KCl, 8.2 mmol/L NaH<sub>2</sub>PO<sub>4</sub>, and 1.25 mmol/L KH<sub>2</sub>PO<sub>4</sub> in 1000 mL of distilled water; pH 7.4). Samples were stored at 37 °C in an incubator for 1, 7, 28, and 56 days. PBS was refreshed every 7 days to replenish the phosphate ions.

**Table 1.** Protooth compositions.

Additives to CSA cement <sup>a</sup> (wt.%)	Fluoride <sup>b</sup>	Radiocontrast	Nano-SiO <sub>2</sub>	Hydration liquid(μl/g powder)	Consistency	Setting time (min)
Protooth	3.5%	10% ZrO <sub>2</sub>	+	190	Creamy	Clay consistency: 4 – 6 Creamy consistency: 8 – 10
Ultrafast Protooth	3.5%	20% ZrO <sub>2</sub>	+	195	Creamy	1½–2
High fluoride Protooth	15%	25%(16% Bi <sub>2</sub> O <sub>3</sub> + 9% SrF <sub>2</sub> )	–	210	Clay-like	8 – 10

<sup>a</sup>CSA composition: tricalcium silicate, dicalcium silicate, Al<sub>2</sub>O<sub>3</sub> < 5% (tricalcium aluminate > 7%), calcium sulfate < 3%, Other components incl. F, PO<sub>4</sub>. Patent Pub. No.: WO 2011/023199.

<sup>b</sup>In all Protooth compositions with 3.5% fluoride additive hereof 1% fluoride was SrF<sub>2</sub>, which also contributes as extra radiocontrast.

In high fluoride Protooth composition with 25% radiocontrast additive hereof 9% was SrF<sub>2</sub>, which also contributes as fluoride additive.

### Scanning electron microscopy and energy dispersive X-ray spectroscopy (SEM/EDX)

The surface changes of sample ultrastructure and morphology were examined with a scanning electron microscope (SEM, CamScan, MaXim 2000, Cambridge, UK) equipped with a secondary electron detector for imaging using an accelerating voltage of 10–20 kV and an EDAX Energy Dispersive System for X-ray analysis using an accelerating voltage of 10 kV. Prior to the SEM/EDX analysis, samples were dried in a desiccator at room temperature. Subsequently, samples were mounted on an aluminum stub and a thin carbon layer was sputter onto the samples surface.

### Raman spectroscopy

Raman spectra were collected using a Witec Confocal Raman Microscope System alpha 300R (Witec Inc., Ulm, Germany). Excitation in the confocal Raman microscopy is assured by a double frequency Nd:YAG laser 532 nm (Newport, Evry, France). The incident laser beam is focused onto the sample through a 20× NIKON objective (Nikon, Tokyo, Japan). Data acquisition is performed using Image Plus software from Witec.

Spectra were acquired on five different areas of the sample of each group. The acquisition time was 90 s. Fresh samples of set cement without PBS immersion were used as control. The apatite intensity was calculated as apatite/belite assigned peak height ratio using a spectral software analysis (WITec Project version 2.06, Witec, Germany).

The data were analyzed by one-way ANOVA (analysis of variance) following Tukey's HSD *post hoc* pairwise comparisons at the significance level of 0.05 using IBM SPSS Statistics 21.0 statistical software.

## Results

### SEM/EDX analysis of Protooth and ultrafast Protooth

SEM analyses revealed surface precipitate with ultrastructure and morphology changes corresponding to the immersion time in PBS. After 1 day, we observed

the formation of spherical and globular precipitates with acicular crystallites (spike-like structure) peripherally and over the samples surface in Protooth (Figure 1) and ultrafast Protooth (Figure 2). After 7 days, more globular precipitations homogenously covered the surface in both groups (Figures 1 and 2). After 28 days, the deposition layer thickened and appeared significantly

more dense in structure with petal-like morphology, which were followed by more compact and voluminous petal-like depositions after 56 days (Figures 1 and 2). EDX analysis revealed the presence of mainly calcium and phosphorus ions in the precipitations indicating the formation of calcium phosphate depositions since day one. Interestingly, heavy atomic strontium peak was

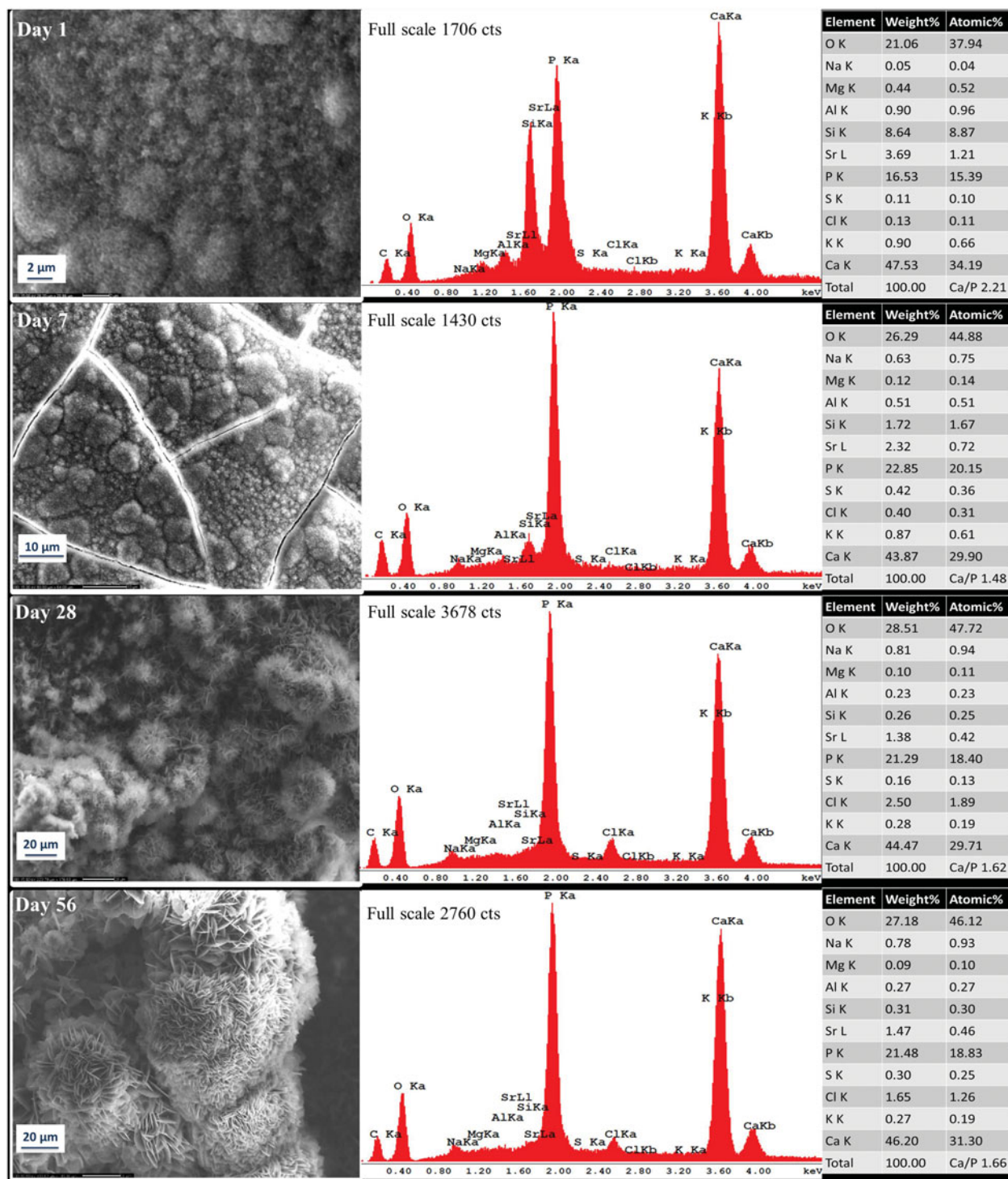


**Figure 1.** Representative morphologic characterization of precipitations formed over Protooth surface immersed in PBS during 56 days. EDX spectrum was obtained from the precipitates in the field of view. Semiquantitative chemical composition presented in the table shows their Ca/P molar ratio.



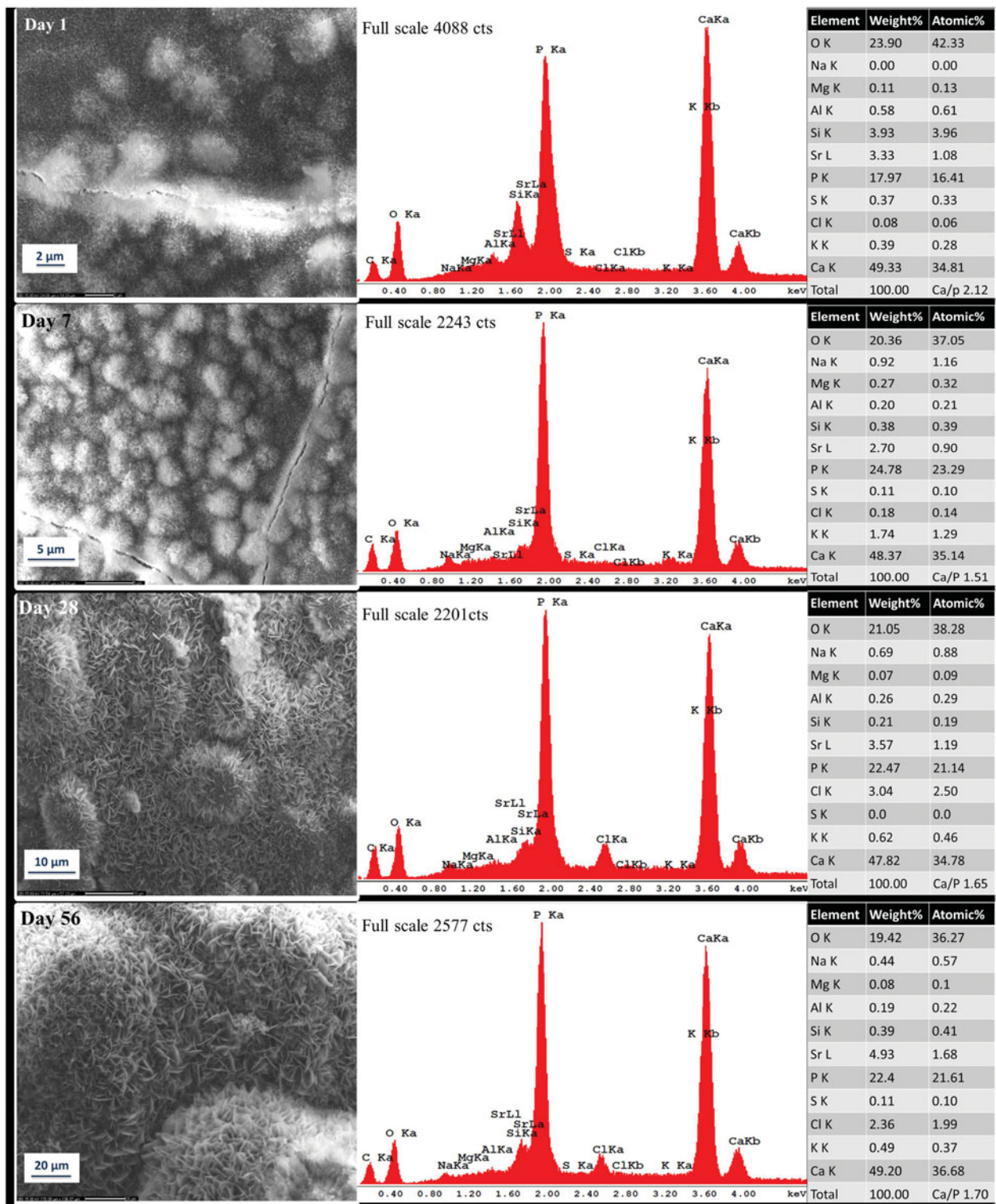


**Figure 2.** Representative morphologic characterization of precipitations formed over ultrafast Protooth surface immersed in PBS during 56 days. EDX spectrum was obtained from the precipitates in the field of view. Semiquantitative chemical composition presented in the table shows their Ca/P molar ratio.

visible in EDX spectra from day 1 to day 56, which can be ascribed to the contribution of strontium ions released by strontium fluoride from the cement. Released fluoride ions with less atomic weight were not detectable in EDX spectra.

Ca/P molar ratio of deposition in the field of view in Protooth (Figure 1) and ultrafast Protooth (Figure 2) after 1 day of aging were 2.21 and 2.12, respectively, decreasing to 1.66 in Protooth and 1.7 in ultrafast Protooth groups for precipitations after 56 days.

### SEM/EDX analysis of high fluoride Protooth

Precipitations in the form of globular aggregates with both acicular and smooth morphology were observed after 1-day immersion in PBS (Figure 3). After 7 days, the entire surface was covered with small globular depositions that homogeneously covered the cement

surface (Figure 3). The compact lath-like precipitations (Figure 3) was formed after 28 days. Compact and denser lath-like depositions continued progressively to form over the surface after 56 days (Figure 3). EDX analysis illustrated majorly calcium and phosphorus ion supporting the formation of calcium phosphate.

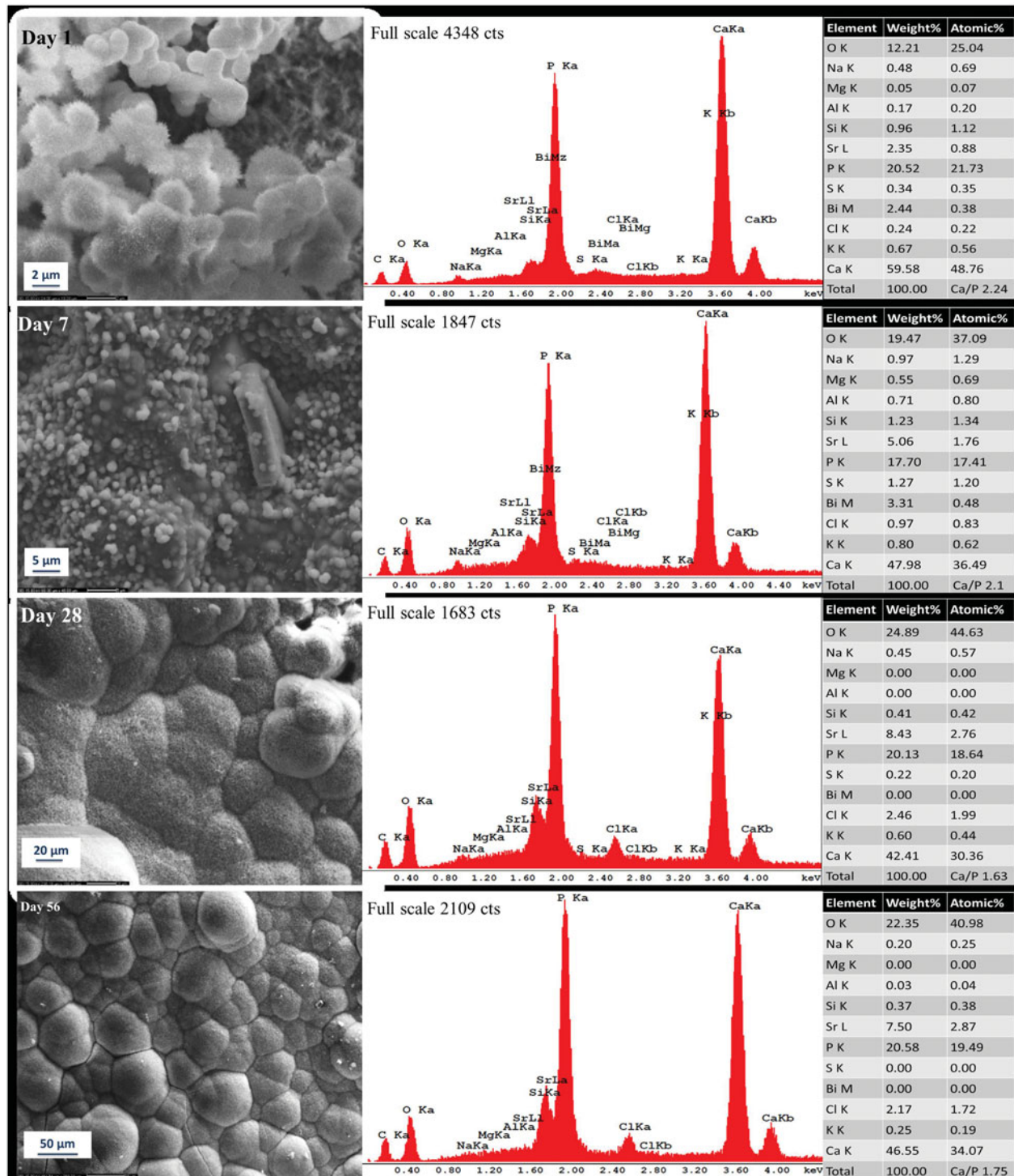


**Figure 3.** Representative morphologic characterization of precipitations formed over high fluoride Protooth surface immersed in PBS during 56 days. EDX spectrum was obtained from the precipitates in the field of view. Semiquantitative chemical composition presented in the table shows their Ca/P molar ratio.

Strontium peaks in precipitations, presumably corresponding to the dissolution of 9% strontium fluoride addition, were visible in EDX spectra in all study time points. Fluoride was not detected in EDX. Ca/P molar ratio of precipitations decreased from 2.24 on day 1 to 1.75 on day 56 corresponding to the representative micrograph in Figure 3 for the field of view.

### Raman analysis

The acquired Raman spectra from the surfaces showed chemical changes when comparing freshly set Protooth to samples after immersion in PBS for 56 days. Raman band assignments were made in accordance with the reported bands in the literature.[14–17] The representative Raman spectra are shown for tested cements in Figure 4(a–c). The intensity ratio of apatite/belite ( $I_{965}/I_{860}$ ) was calculated as an indicator of apatite precipitations thickness (Figure 4(d)). Table 2 reports the wavenumbers and assignments of the vibrational bands corresponding to the apatite deposition on the sample surface after 56-day immersion in PBS.

### Raman analysis of Protooth and ultrafast Protooth

Acquired Raman spectra for Protooth and ultrafast Protooth were almost similar (Figure 4(a) and (b)). A representative spectrum of Protooth and ultrafast Protooth surface characterization is shown in Figure 4(a and b), respectively. The recorded spectra from set Protooth and ultrafast Protooth samples disclosed a range of bands from  $180\text{ cm}^{-1}$  to  $638\text{ cm}^{-1}$  assigned to monoclinic zirconium oxide ( $180, 192, 224, 280, 308, 335, 349, 384, 455, 477, 503, 513, 539, 561, 590, 618, \text{ and } 638\text{ cm}^{-1}$ ). Bands of anhydrite ( $1019\text{ cm}^{-1}$  attributed to  $\nu_1\text{ SO}_4^{2-}$ ), alite ( $848\text{ cm}^{-1}$ ,  $\nu_1\text{ SiO}_4^{4-}$ ), belite ( $848\text{ cm}^{-1}$  and  $860\text{ cm}^{-1}$  assigned to  $\nu_1\text{ SiO}_4^{4-}$ ), and calcium carbonate in the form of calcite and/or aragonite ( $1090\text{ cm}^{-1}$ ,  $\nu_1\text{ CO}_3^{2-}$  stretching mode) was detectable for set materials. The presence of Raman band at  $970\text{ cm}^{-1}$  attributed to the  $\nu_1\text{ PO}_4^{3-}$  from the set cement supports the presence of phosphate in the composition of Protooth and ultrafast Protooth. After 1 day, the band at  $965\text{ cm}^{-1}$ , assigned to the  $\nu_1$  stretching mode of  $\text{PO}_4^{3-}$  was found over the cement surface. The presence of this band suggests the formation of an apatite layer on the sample surface.[14,16] The intensity of alite in respect to belite has been decreased due to faster hydration rate of alite.[18] The other cements bands for zirconium oxide, calcium carbonate, and anhydrite were still detectable.

After 7 days, bands of calcium carbonate and anhydrite were dimmed. The intensity of apatite band

at  $965\text{ cm}^{-1}$  was increased in respect to belite band ( $860\text{ cm}^{-1}$ ). New Raman shift at  $435\text{ cm}^{-1}$  assigned to  $\nu_2\text{ PO}_4^{3-}$  bending mode was visible. Appearance of small peaks at the range of  $1022$  to  $1080\text{ cm}^{-1}$  ascribed to  $\nu_3\text{ PO}_4^{3-}$  asymmetric stretching mode [19–21] in ultrafast Protooth was observed.

After 28 days, thickened superficial apatite layer exhibited a more intense band of  $\text{PO}_4^{3-}$  at  $435$  and  $965\text{ cm}^{-1}$  in respect to cement bend (belite). Bands associated with alite and anhydrite became weaker and disappeared. We found the bands at the range of  $1022$ – $1080\text{ cm}^{-1}$  with peaks at  $1022, 1048, \text{ and } 1077\text{ cm}^{-1}$  ascribed to  $\nu_3\text{ PO}_4^{3-}$  asymmetric stretching mode. The peak at  $1077\text{ cm}^{-1}$  has been assigned to either the phosphate  $\nu_3$  mode or the carbonate  $\nu_1$  mode or both. Hence, the pattern of Raman bands after 28 days supported the formation of  $\beta$ -type carbonated apatite on the Protooth and ultrafast Protooth surface. The same peaks at  $435, 965, 1022, 1048, \text{ and } 1077\text{ cm}^{-1}$  with a higher intensity in respect to belite were detected on day 56, which suggest the progressive and thicker superficial apatite layer formation. Note that because of  $\text{ZrO}_2$  Raman bands superimposition, the bands for  $\nu_4\text{ PO}_4^{3-}$  bending mode of apatite at the range of  $590$ – $610\text{ cm}^{-1}$  was not detectable.

### Raman analysis of high fluoride Protooth

Raman spectra in high fluoride Protooth revealed different radiocontrast element in comparison to Protooth and ultrafast Protooth (Figure 4(c)). Raman shifts at  $189, 214, 280, 295, 318, 409, \text{ and } 452\text{ cm}^{-1}$  affirmed the presence of bismuth oxide in high fluoride Protooth composition. Raman shifts detected alite and belite at  $526$  and  $540\text{ cm}^{-1}$  assigned to  $\nu_4\text{ SiO}_4^{4-}$ ,  $836$  and  $848\text{ cm}^{-1}$  assigned to  $\nu_1\text{ SiO}_4^{4-}$ . An intense marker peak of monoclinic belite at  $860\text{ cm}^{-1}$  attributed to  $\nu_1\text{ SiO}_4^{4-}$  were also found in set high fluoride Protooth. Calcium carbonate (calcite and/or aragonite) and anhydrite were identified by peaks at  $1090\text{ cm}^{-1}$  ( $\nu_1\text{ CO}_3^{2-}$  stretching mode) and  $1019\text{ cm}^{-1}$  ( $\nu_1\text{ SO}_4^{2-}$  stretching mode), respectively.

The intensity of band assigned to alite, calcite, and anhydrite were decreased with respect to belite after 1 day. Appearance of bands at  $592\text{ cm}^{-1}$  assigned to  $\nu_4\text{ PO}_4^{3-}$  bending mode and  $965\text{ cm}^{-1}$  assigned to the  $\nu_1\text{ PO}_4^{3-}$  stretching mode of phosphate, suggested the formation of superficial apatite layer. Vaterite symmetric stretching mode ( $\nu_1\text{ CO}_3^{2-}$ ) was observed at  $1075\text{ cm}^{-1}$ . After 7 days, increased intensity of bands associated with apatite, accompanied by the rise of the band at  $1077\text{ cm}^{-1}$  ascribed to phosphate and carbonate group support the formation of  $\beta$ -type



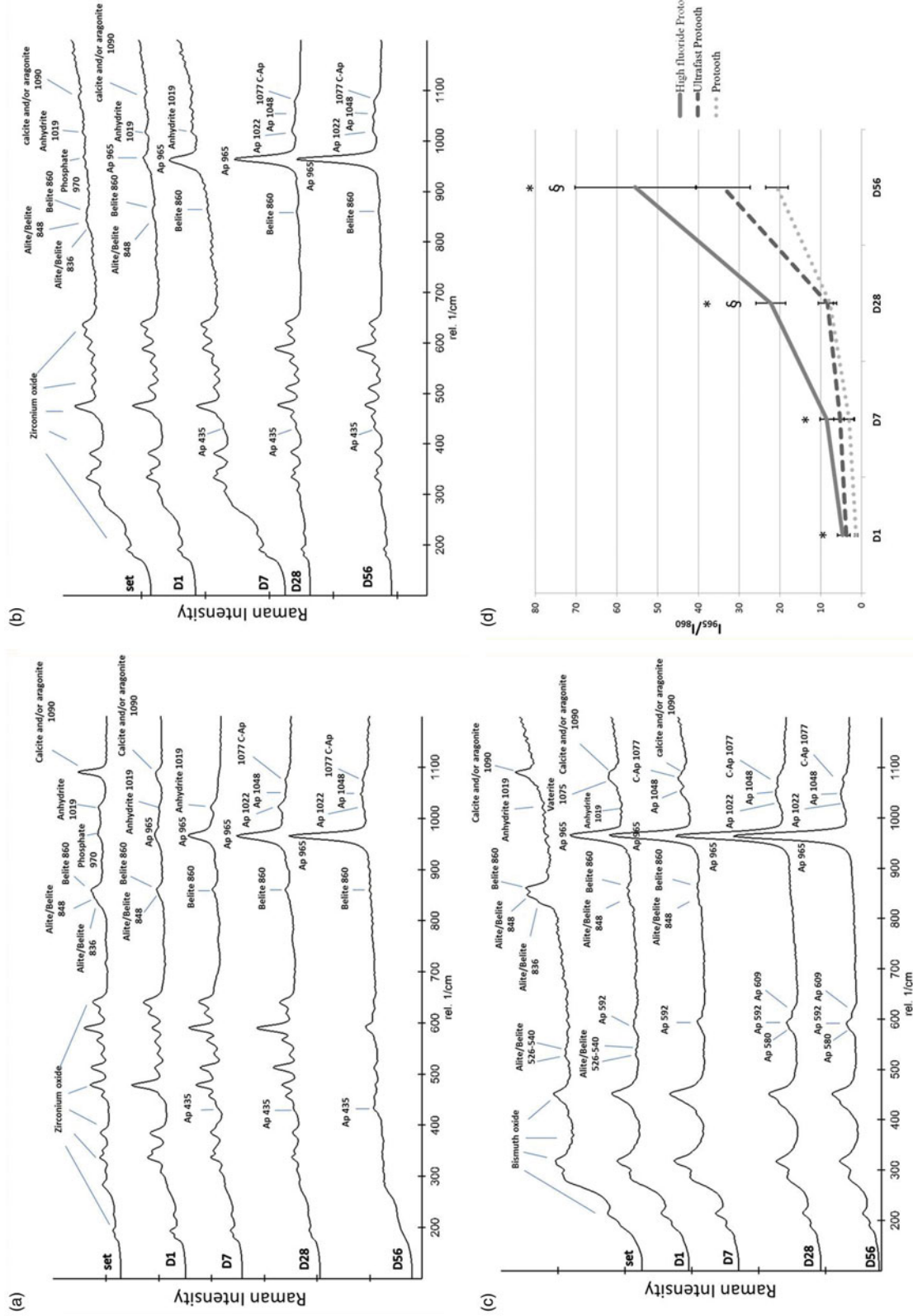


**Figure 4.** Representative Raman spectra recorded on the surface of Protooth (a), ultrafast Protooth (b), and high fluoride Protooth (c) as the function of immersion time in PBS. The corresponding bands to apatite has been indicated with Ap and C-Ap ( $\beta$ -type carbonated apatite).  $I_{965}/I_{860}$  intensity ratio (apatite/belite) obtained from the spectra recorded on the surface of all Protooth compositions immersed in PBS as a function of time (d). A higher intensity ratio is related to thicker apatite deposition. \* denotes a significant difference between Protooth and high fluoride Protooth at each time point. § denotes a significant difference between ultrafast Protooth and high fluoride Protooth at each time point. All cements showed statistically significant increase after 56 days compared to day 1 ( $p < 0.0001$ ).

**Table 2.** Raman shift wavenumbers ( $\text{cm}^{-1}$ ) and bands assignments of apatite recorded on the surface of the cements after 56 days.

Wavenumber ( $\text{cm}^{-1}$ )	Vibrational mode	Crystal phase	Cement
1077	$\nu_1 \text{CO}_3^{2-}$ symmetric stretching	$\beta$ -type carbonated apatite	Protooth Ultrafast Protooth High fluoride Protooth
1048	$\nu_3 \text{PO}_4^{3-}$ asymmetric stretching	Apatite	Protooth Ultrafast Protooth High fluoride Protooth
1022	$\nu_3 \text{PO}_4^{3-}$ asymmetric stretching	Apatite	Protooth Ultrafast Protooth High fluoride Protooth
965	$\nu_1 \text{PO}_4^{3-}$ symmetric stretching	Apatite	Protooth Ultrafast Protooth High fluoride Protooth
609	$\nu_4 \text{PO}_4^{3-}$ bending	Apatite	High fluoride (superimposed with zirconium oxide in Protooth and ultrafast Protooth)
592	$\nu_4 \text{PO}_4^{3-}$ bending	Apatite	High fluoride (superimposed with zirconium oxide in Protooth and ultrafast Protooth)
580	$\nu_4 \text{PO}_4^{3-}$ bending	Apatite	High fluoride (superimposed with zirconium oxide in Protooth and ultrafast Protooth)
435	$\nu_2 \text{PO}_4^{3-}$ bending	Apatite	Protooth Ultrafast Protooth (superimposed with bismuth oxide in high fluoride Protooth)

carbonate apatite. In Raman spectra, a small shoulder at  $1090 \text{ cm}^{-1}$  from calcium carbonate was still detectable but anhydrite was not detectable after 7 days. Bands at  $580$  and  $609 \text{ cm}^{-1}$  assigned to  $\nu_4 \text{PO}_4^{3-}$  and  $1022$  and  $1048 \text{ cm}^{-1}$  assigned to  $\nu_3 \text{PO}_4^{3-}$  bending mode were disclosed after 28 days. The peaks for anhydrite, calcite and/or aragonite, and alite were not visible. The intensity of apatite bands ( $580$ ,  $591$ ,  $609$ ,  $965$ ,  $1022$ ,  $1045$ , and  $1077 \text{ cm}^{-1}$ ) were raised with respect to belite ( $860 \text{ cm}^{-1}$ ) after 56 days. Because of bismuth oxide Raman shift superimposition within the range of  $189$  to  $455 \text{ cm}^{-1}$ ,  $\nu_2 \text{PO}_4^{3-}$  of apatite was not detectable in high fluoride Protooth.

The Raman peak intensity ratio between apatite ( $965 \text{ cm}^{-1}$ ) to belite ( $860 \text{ cm}^{-1}$ ), which has been considered as indicator for apatite formation thickness, revealed the progressive increase in this ratio in all Protooth compositions. All cements showed significant increase following immersion in PBS after 56 days compared to 1-day precipitations ( $p < 0.0001$ ), suggesting thicker apatite formation on the surface of all Protooth compositions as the function of time in PBS (Figure 4(d)). Ultrafast Protooth had higher apatite/belite ratio in comparison with Protooth only on 1-day precipitations ( $p = 0.004$ ). High fluoride Protooth showed significantly higher apatite/belite ratio against Protooth at all study time points and against ultrafast Protooth after 28 and 56 days, suggesting thicker apatite deposition over high fluoride Protooth.

## Discussion

This study demonstrated that a novel fast-setting calcium silicate cement (Protooth) can form a superficial

apatite layer after immersion in PBS. The privileged success and performance of MTA is attributed to form superficial bone-like apatite layer in contact with a physiological-like solution.[1,2] The hydration reaction of calcium silicate (dicalcium and tricalcium silicate) with considerable amount of calcium oxide groups in the cement composition results in CH release and pH rise.[12] The substantial release of  $\text{Ca}^{2+}$  and  $\text{OH}^-$  ions in solution with a high amount of phosphate, as in physiological liquids, cause supersaturation with respect to apatite, which ultimately precipitates in the presence of nucleation site.[22] Fluoride-doped calcium silicate cement has demonstrated accelerated superficial apatite formation with the earlier formation of fluorapatite.[23] Silanol groups in calcium silicate hydrate gel can act as a nucleation site for calcium phosphate precipitations in calcium silicate cement.[24,25] Formation of amorphous calcium phosphate as apatite precursor undergoes phase transformation into carbonated apatite over time.[26]

We used Raman spectroscopy as a complementary method to SEM/EDX to assess the formed precipitations on the surface of Protooth throughout the experiment time to elicit the chemical composition of unique phases. The usability and reliability of Raman spectroscopy for apatite characterization has been demonstrated in several studies.[16,17,27] In this study, we compared three different Protooth compositions with various radiocontrast and fluoride content.

All Protooth compositions showed the formation of calcium phosphate precipitations (apatite) after 1 day immersing in PBS. The formed apatite layer in ultrafast Protooth was in average higher, with no significant difference, in apatite-to-belite Raman peak intensity



ratio in comparison with Protooth after 56 days (Figure 4(d)). The solubility of calcium silicate cement with the same liquid-to-powder ratio can increase as the function of radiocontrast.[28] On the other hand, the concentration of released and accessible ions influence the nucleation and precipitation of apatite.[29] Thus, it can be speculated that slightly more ions can be released from ultrafast Protooth rather than Protooth, which may explain the higher apatite-forming ability of ultrafast Protooth. However, elevated additive material causes reduction in cement quantity. Further study to address the solubility and ion release of Protooth are needed.

Precipitations on the three Protooth compositions showed Ca/P ratio above 2 after 1 day because of calcium carbonate formation (Raman band at  $1090\text{ cm}^{-1}$ ) in the form of calcite and/or aragonite.[16] Calcium carbonate can form because of calcium ions reaction with environmental carbonate ions. After 7 days, calcium carbonate was not detectable in Raman (except in high fluoride Protooth), which caused drop at Ca/P ratio in EDX spectra revealing Ca-poor apatite [30] over the surface of Protooth and ultrafast Protooth. Ca/P ratio in EDX spectra and appearance of other phosphate vibrational modes in Raman spectra particularly band at  $1077\text{ cm}^{-1}$  can support the formation of  $\beta$ -type carbonated apatite in all groups after 28 days. It has been well-documented that presence of Raman band at  $1077\text{ cm}^{-1}$  is the marker band for  $\beta$ -type carbonated apatite in Raman spectra.[14,17,27] Carbonated apatite represents the mineral phase of hard tissues such as bone, cementum, and dentin and is known as a biologic apatite.[1] Protooth compositions possessed more compact and voluminous deposition in morphology after 56 days compared to precipitations after 1 day. Our findings are consistent with other studies showing that more compact calcium phosphate structures were prominent after longer time in PBS. Compact precipitation structures possess higher Ca/P ratio in comparison with needle-like and acicular calcium phosphate deposits.[1,31,32]

Raman spectra of set Protooth and ultrafast Protooth, disclosed the presence of phosphate phase (Raman band at  $970\text{ cm}^{-1}$ ) in the composition of the set cement. Phosphate groups with negatively charged over the cement surface can act as a nucleation site to improve and accelerate the kinetics of apatite formation.[30]

In this study, high fluoride Protooth showed significantly higher apatite-to-belite Raman peak intensity ratio after 28 and 56 days compared to other two compositions (Figure 4(d)). Higher radiocontrast and

fluoride content may cause higher solubility and higher ion release from high fluoride Protooth, which can enhance the apatite formation. Gandolfi et al.[23] assessed the apatite formation ability of fluoride-containing calcium silicate cements. They concluded that presence of fluoride in the composition of the cement increases the apatite-forming ability and additionally lead to the formation of fluorapatite. F-substituted apatite can act as a new nucleation site for apatite layer by incorporation of  $\text{Ca}^{2+}$ ,  $\text{PO}_4^{3-}$ , and  $\text{F}^-$  ions. Fluoride is the most electronegative element, and it has a strong affinity for exchange with hydroxyl ion in hydroxyapatite.[33] Fluoride ion substitution modifies the structure or crystal lattice and reduces the dissolution properties of apatite. The lower solubility of fluorapatite compared to hydroxyapatite enhances the tooth structure mineral resistance against caries in an acidic pH.[34] Fluoride ions at the tooth surface even at low concentrations have been shown to interfere with the initiation and progression of caries lesions. When pH in dental plaque drops below critical pH (c.a 5.5), apatite mineralization and remineralization process can take place in the presence of fluoride ions. So, fluoride ions can enhance the mineralization and remineralization process.[35] Long-term fluoride ions release from Protooth compositions has been measured at the ppm level (unpublished data). Detection of fluoride substituted apatite or fluorapatite was not possible in this study. The sensitivity of EDX and Raman spectroscopy in the detection of the fluoridation degree of apatite deposit particularly in low concentration may explain the methodological limitation of the study.[23] Partially fluoridated hydroxyapatite, with the substitution of  $\text{OH}^-$  with  $\text{F}^-$ , has almost similar Raman spectra as hydroxyapatite.[36] Other complementary characteristic methods are needed to investigate the influence of fluoride presence on precipitation.

Interestingly, our acquired EDX spectra in all Protooth compositions revealed the presence of heavy strontium atoms with high signal over the samples surface precipitations. This is indicating that strontium ions from strontium fluoride in Protooth compositions have been released and redistributed. The strontium EDX peak was detectable over cement surface, which may suggest the substitution of  $\text{Ca}^{2+}$  ions by strontium in the composition of superficial apatite.

The apatite-forming ability of dental material may be considered as a basis and indicator for the biocompatibility of biomaterials.[22] Superficial apatite formation may introduce a suitable surface for cells that can stimulate odontoblast-like cells.[37,38] Apatite formation can also be favorable in term of remineralizing the

adjacent dentin through the intrafibrillar deposition of apatite crystals [39] and increase the material bonding to dentin.[40] Furthermore, apatite precipitation can form inside the dentinal tubules along the material–dentin interface [1] and improve the sealing potential,[3] which may address the advantageous clinical performance of calcium silicate cement.

The hydrophilic nature of the novel calcium silicate cement (Protooth) in contrast to the humidity sensitive dental materials like glass ionomers may be an advantage in challenging humid conditions in the oral cavity. The release of ions from Protooth, which as shown in this study can support apatite formation, may also support mineralization or remineralization in tooth structure. This could be relevant for clinical caries control aspects in preventive dentistry.

The results of the present study suggest that all Protooth compositions possess the ability to form apatite precipitation in PBS. The formed apatite layer in all Protooth groups can thicken as the function of time. High fluoride Protooth can form thicker apatite precipitations. Further studies regarding biocompatibility and dentin/enamel remineralization ability of Protooth seem relevant.

## Acknowledgements

We thank Javier Garcia for the assistance in this study.

## Disclosure statement

Henrik Løvschall as patentee has financial relation with Dentosolve. The other authors declare that they have no conflict of interest.

## References

- [1] Reyes-Carmona JF, Felipe MS, Felipe WT. Biomineralization ability and interaction of mineral trioxide aggregate and white Portland cement with dentin in a phosphate-containing fluid. *J Endod.* 2009;35:731–736.
- [2] Sarkar NK, Caicedo R, Ritwik P, et al. Physicochemical basis of the biologic properties of mineral trioxide aggregate. *J Endod.* 2005;31:97–100.
- [3] Martin RL, Monticelli F, Brackett WW, et al. Sealing properties of mineral trioxide aggregate orthograde apical plugs and root fillings in an in vitro apexification model. *J Endod.* 2007;33:272–275.
- [4] Eldeniz AU, Hadimli HH, Ataoglu H, et al. Antibacterial effect of selected root-end filling materials. *J Endod.* 2006;32:345–349.
- [5] Kogan P, He J, Glickman GN, et al. The effects of various additives on setting properties of MTA. *J Endod.* 2006;32:569–572.
- [6] Hsieh SC, Teng NC, Lin YC, et al. A novel accelerator for improving the handling properties of dental filling materials. *J Endod.* 2009;35:1292–1295.
- [7] Formosa LM, Mallia B, Camilleri J. A quantitative method for determining the antiwashout characteristics of cement-based dental materials including mineral trioxide aggregate. *Int Endod J.* 2013;46:179–186.
- [8] Huang TH, Shie MY, Kao CT, et al. The effect of setting accelerator on properties of mineral trioxide aggregate. *J Endod.* 2008;34:590–593.
- [9] Bortoluzzi EA, Broon NJ, Bramante CM, et al. The influence of calcium chloride on the setting time, solubility, disintegration, and pH of mineral trioxide aggregate and white Portland cement with a radiopacifier. *J Endod.* 2009;35:550–554.
- [10] Lee BN, Hwang YC, Jang JH, et al. Improvement of the properties of mineral trioxide aggregate by mixing with hydration accelerators. *J Endod.* 2011;37:1433–1436.
- [11] Gemalmaz D, Yoruc B, Ozcan M, et al. Effect of early water contact on solubility of glass ionomer luting cements. *J Prosthet Dent.* 1998;80:474–478.
- [12] Camilleri J. Hydration mechanisms of mineral trioxide aggregate. *Int Endod J.* 2007;40:462–470.
- [13] Parirokh M, Torabinejad M. Mineral trioxide aggregate: a comprehensive literature review – Part III: clinical applications, drawbacks, and mechanism of action. *J Endod.* 2010;36:400–413.
- [14] Nelson DG, Featherstone JD. Preparation, analysis, and characterization of carbonated apatites. *Calcif Tissue Int.* 1982;34:S69–S81.
- [15] Tarrida M, Madon M, Le Rolland B, et al. An in-situ Raman spectroscopy study of the hydration of tricalcium silicate. *Adv Cem Based Mater.* 1995;2:15–20.
- [16] Taddei P, Tinti A, Gandolfi MG, et al. Ageing of calcium silicate cements for endodontic use in simulated body fluids: a micro-Raman study. *J Raman Spectrosc.* 2009;40:1858–1866.
- [17] Gandolfi M, Taddei P, Tinti A, et al. Kinetics of apatite formation on a calcium-silicate cement for root-end filling during ageing in physiological-like phosphate solutions. *Clin Oral Investig.* 2010;14:659–668.
- [18] Martinez-Ramirez S, Frías M, Domingo C. Micro-Raman spectroscopy in white Portland cement hydration: long-term study at room temperature. *J Raman Spectrosc.* 2006;37:555–561.
- [19] Awonusi A, Morris MD, Tecklenburg MM. Carbonate assignment and calibration in the Raman spectrum of apatite. *Calcif Tissue Int.* 2007;81:46–52.
- [20] Iqbal Z, Tomaselli VP, Fahrenfeld O, et al. Polarized Raman scattering and low frequency infrared study of hydroxyapatite. *J Phys Chem Solids.* 1977;38:923–927.
- [21] de Aza PN, Guitián F, Santos C, et al. Vibrational properties of calcium phosphate compounds. 2. Comparison between hydroxyapatite and  $\beta$ -tricalcium phosphate. *Chem Mater.* 1997;9:916–922.
- [22] Kokubo T, Takadama H. How useful is SBF in predicting in vivo bone bioactivity? *Biomaterials.* 2006;27:2907–2915.
- [23] Gandolfi MG, Taddei P, Siboni F, et al. Fluoride-containing nanoporous calcium-silicate MTA cements

- for endodontics and oral surgery: early fluorapatite formation in a phosphate-containing solution. *Int Endod J.* 2011;44:938–949.
- [24] Labbez C, Jönsson B, Pochard I, et al. Surface charge density and electrokinetic potential of highly charged minerals: experiments and monte carlo simulations on calcium silicate hydrate. *J Phys Chem B.* 2006; 110:9219–9230.
- [25] Liu X, Ding C, Chu PK. Mechanism of apatite formation on wollastonite coatings in simulated body fluids. *Biomaterials.* 2004;25:1755–1761.
- [26] Tay FR, Pashley DH, Rueggeberg FA, et al. Calcium phosphate phase transformation produced by the interaction of the Portland cement component of white mineral trioxide aggregate with a phosphate-containing fluid. *J Endod.* 2007;33:1347–1351.
- [27] Gandolfi MG, Taddei P, Tinti A, et al. Apatite-forming ability (bioactivity) of ProRoot MTA. *Int Endod J.* 2010;43:917–929.
- [28] Cutajar A, Mallia B, Abela S, et al. Replacement of radiopacifier in mineral trioxide aggregate; characterization and determination of physical properties. *Dent Mater.* 2011;27:879–891.
- [29] Weng J, Liu Q, Wolke JG, et al. Formation and characteristics of the apatite layer on plasma-sprayed hydroxyapatite coatings in simulated body fluid. *Biomaterials.* 1997;18:1027–1035.
- [30] Gandolfi MG, Taddei P, Tinti A, et al. Alpha-TCP improves the apatite-formation ability of calcium-silicate hydraulic cement soaked in phosphate solutions. *Mater Sci Eng C.* 2011;31:1412–1422.
- [31] Han L, Okiji T, Okawa S. Morphological and chemical analysis of different precipitates on mineral trioxide aggregate immersed in different fluids. *Dent Mater J.* 2010;29:512–517.
- [32] Han L, Okiji T. Bioactivity evaluation of three calcium silicate-based endodontic materials. *Int Endod J.* 2013;46:808–814.
- [33] Kay MI, Young RA, Posner AS. Crystal structure of hydroxyapatite. *Nature.* 1964;204:1050–1052.
- [34] Fulmer MT, Ison IC, Hankermayer CR, et al. Measurements of the solubilities and dissolution rates of several hydroxyapatites. *Biomaterials.* 2002;23: 751–755.
- [35] Fejerskov O, Larsen MJ, Richards A, et al. Dental tissue effects of fluoride. *Adv Dent Res.* 1994;8:15–31.
- [36] Campillo M, Lacharaise PD, Reparaz JS, et al. On the assessment of hydroxyapatite fluoridation by means of Raman scattering. *J Chem Phys.* 2010;132:244501–244505
- [37] Gandolfi MG, Ciapetti G, Taddei P, et al. Apatite formation on bioactive calcium-silicate cements for dentistry affects surface topography and human marrow stromal cells proliferation. *Dent Mater.* 2010;26: 974–992.
- [38] Gandolfi MG, Shah SN, Feng R, et al. Biomimetic calcium-silicate cements support differentiation of human orofacial mesenchymal stem cells. *J Endod.* 2011;37:1102–1108.
- [39] Tay FR, Pashley DH. Guided tissue remineralisation of partially demineralised human dentine. *Biomaterials.* 2008;29:1127–1137.
- [40] Reyes-Carmona JF, Felipe MS, Felipe WT. The biomineralization ability of mineral trioxide aggregate and Portland cement on dentin enhances the push-out strength. *J Endod.* 2010;36:286–291.